

# First detection of glycolaldehyde outside the Galactic Center<sup>1</sup>

M. T. Beltrán<sup>2</sup>, C. Codella<sup>3</sup>, S. Viti<sup>4</sup>, R. Neri<sup>5</sup>, R. Cesaroni<sup>6</sup>

## ABSTRACT

Glycolaldehyde is the simplest of the monosaccharide sugars and is directly linked to the origin of life. We report on the detection of glycolaldehyde (CH<sub>2</sub>OHCHO) towards the hot molecular core G31.41+0.31 through IRAM PdBI observations at 1.4, 2.1, and 2.9 mm. The CH<sub>2</sub>OHCHO emission comes from the hottest ( $\geq 300$  K) and densest ( $\geq 2 \times 10^8$  cm<sup>-3</sup>) region closest ( $\leq 10^4$  AU) to the (proto)stars. The comparison of data with gas-grain chemical models of hot cores suggests for G31.41+0.31 an age of a few  $10^5$  yr. We also show that only small amounts of CO need to be processed on grains in order for existing hot core gas-grain chemical models to reproduce the observed column densities of glycolaldehyde, making surface reactions the most feasible route to its formation.

*Subject headings:* ISM: individual objects: G31.41+0.31 — ISM: molecules — stars: formation

## 1. Introduction

Glycolaldehyde (CH<sub>2</sub>OHCHO), an isomer of both methyl formate (HCOOCH<sub>3</sub>) and acetic acid (CH<sub>3</sub>COOH), is the simplest of the monosaccharide sugars. The importance of this organic molecule is that it can react with propenal to form ribose, a central constituent of

---

<sup>1</sup>Based on observations carried out with the IRAM Plateau de Bure Interferometer. IRAM is supported by INSU/CNRS (France), MPG (Germany) and IGN (Spain).

<sup>2</sup>Universitat de Barcelona, Departament d'Astronomia i Meteorologia, Unitat Associada a CSIC, Martí i Franquès, 08028 Barcelona, Catalunya, Spain; mbeltran@am.ub.es

<sup>3</sup>INAF, Istituto di Radioastronomia, Sezione di Firenze, Largo E. Fermi 5, I-50125 Firenze, Italy; codella@arcetri.astro.it

<sup>4</sup>Department of Physics and Astronomy, University College London, Gower Street, London WC1E6BT, UK; sv@star.ucl.ac.uk

<sup>5</sup>IRAM, 300 Rue de la Piscine, F-38406 Saint Martin d'Hères, France; neri@iram.fr

<sup>6</sup> INAF, Osservatorio Astrofisico di Arcetri, Largo E. Fermi 5, I-50125 Firenze, Italy; cesa@arcetri.astro.it

RNA, and is, therefore, directly linked to the origin of life. Hence, it is crucial to investigate the occurrence of glycolaldehyde in the universe, especially in star-forming regions, where stars associated with planetary systems are expected to form. Interstellar glycolaldehyde has first been detected towards the Galactic center source Sgr B2(N) by Hollis et al. (2000), and successively confirmed by Halfen et al. (2006) and Requena-Torres et al. (2008), through single-dish observations. Interferometric observations (Hollis et al. 2001) of the Sgr B2(N) region, known as the Large Molecule Heimat (LMH), have shown that, unlike its isomers methyl formate and acetic acid, glycolaldehyde has a large spatial scale,  $60''$ .

Beltrán et al. (2005) have reported the detection of a bright line at 220.46 GHz, observed with the IRAM Plateau de Bure Interferometer (PdBI), towards the massive star-forming regions G31.41+0.31 and G24.78+0.08. In the latter case, such a line has been detected in two distinct cores, A1 and A2. This emission has been interpreted as possibly arising from the transition  $20_{2,18}-19_{3,17}$  of  $\text{CH}_2\text{OHCHO}$ . However, it should be noted that a single tentative detection of an interstellar molecule transition is not enough for establishing its identification (Snyder et al. 2005). We have performed an observational campaign to detect multiple transitions of  $\text{CH}_2\text{OHCHO}$  in G31.41+0.31 in order to confirm for the first time the presence of glycolaldehyde in a compact core in a star forming region, possibly associated with the material assembling the newly born massive protostars.

G31.41+0.31 is a very massive star-forming region located at a distance of 7.9 kpc (Churchwell, Walmsley, & Cesaroni 1990), associated with a hot ( $T \simeq 300$  K) molecular core (HMC), with a luminosity of  $\sim 3 \times 10^5 L_\odot$  and thought to be heated by one or more O-B (proto)stars. Beltrán et al. (2004) have detected a clear velocity gradient perpendicular to the direction of a bipolar outflow imaged by Olmi et al. (1996) at the center of the core (see Fig. 2). Such a velocity gradient has been interpreted as rotation of a massive toroid ( $M_{\text{gas}} \sim 490 M_\odot$ ) about the axis of the outflow. In addition, recent SMA interferometric observations at 226 GHz have detected CN and  $\text{H}_2\text{CO}$  in red-shifted absorption towards the dust continuum of the hot core (Beltrán et al., in preparation), which indicates the presence of accretion in such a massive toroid. Therefore, G31.41+0.31 very much resembles the  $20 M_\odot$  young stellar object G24.78+0.08 A1, where infall, outflow, and rotation have been simultaneously detected for the first time towards a massive (proto)star (Beltrán et al. 2006).

In this letter, we report the first detection of glycolaldehyde towards a HMC located outside the Galactic center, and show that there is a viable mechanism for glycolaldehyde to be abundant in HMCs by means of chemical modelling.

## 2. Observations

We carried out observations at 1.4, 2.1, and 2.9 mm with the PdBI on March 2003, June 2008, and July 2008, respectively. Line data have a spectral resolution of 3.4, 0.33, and 0.45 km s<sup>-1</sup> at 1.4, 2.1, and 2.9 mm, respectively. Channel maps were created with natural weighting, obtaining synthesized beams and 1 $\sigma$  RMS of 1''.1 $\times$ 0''.5 and 50 mJy/beam/channel at 1.4 mm, 4''.1 $\times$ 3''.2 and 13 mJy/beam/channel at 2.1 mm, and 5''.4 $\times$ 4''.4 and 9 mJy/beam/channel at 2.9 mm.

## 3. Detection of glycolaldehyde

Figure 1 reports the spectra observed at 1.4, 2.1, and 2.9 mm towards the peak position of the HMC G31.41+0.31. As can be seen in the top panel, besides the CH<sub>3</sub>CN (12<sub>8</sub>–11<sub>8</sub>) and CH<sub>3</sub><sup>13</sup>CN (12<sub>6</sub>–11<sub>6</sub>) transitions, other lines are detected. In particular, there is a clear emission peak at 220465.86 MHz. Although the line is blended with the CH<sub>3</sub>CN (12<sub>8</sub>–11<sub>8</sub>) and CH<sub>3</sub><sup>13</sup>CN (12<sub>6</sub>–11<sub>6</sub>) transitions, there is no doubt of the presence of a separate line at 220465.86 MHz. On the basis of the Jet Propulsion Laboratory, Cologne, and Lovas databases for molecular spectroscopy, the only possible identification is the CH<sub>2</sub>OHCHO (20<sub>2,18</sub>–19<sub>3,17</sub>) line at 220463.87 MHz ( $E_u=120$  K;  $S\mu^2 = 65.39$  D<sup>2</sup>). The difference between the observed and the laboratory frequencies ( $\sim 1.99$  MHz), albeit non negligible, is less than the spectral resolution of 2.50 MHz. Such a discrepancy is not surprising since it has been found in several glycolaldehyde transitions observed towards Sgr B2(N) (Hollis et al. 2000; Halfen et al. 2006) and could reflect the uncertainties on the CH<sub>2</sub>OHCHO rest frequencies in the spectral catalogues. As mentioned above, the glycolaldehyde 20<sub>2,18</sub>–19<sub>3,17</sub> line is blended with two molecular transitions of CH<sub>3</sub>CN and CH<sub>3</sub><sup>13</sup>CN. Beltrán et al. (2005) fitted the three lines with Gaussians having the same line width (FWHM), and separations in frequency identical to the laboratory values (allowing for the above mentioned difference of 1.99 MHz for the glycolaldehyde transition). Here, we prefer instead to leave all parameters free to allow for possible differences in the FWHM of different molecules and for the sake of consistency with the method adopted to fit the other two glycolaldehyde lines (see below). The new value of the FWHM of the 1.4 mm line is  $9.2\pm 0.7$  km s<sup>-1</sup>.

To confirm the tentative detection of glycolaldehyde, we checked for other CH<sub>2</sub>OHCHO lines that have already been detected towards the Galactic center. Based on the Galactic center CH<sub>2</sub>OHCHO survey performed at 2 mm and 3 mm by Halfen et al. (2006), we observed towards G31.41+0.31 the CH<sub>2</sub>OHCHO (10<sub>1,9</sub>–9<sub>2,8</sub>) and (14<sub>0,14</sub>–13<sub>1,13</sub>) transitions respectively at 103667.907 MHz ( $E_u=32$  K;  $S\mu^2 = 26.22$  D<sup>2</sup>) and 143640.936 MHz ( $E_u=53$  K;  $S\mu^2 = 67.56$  D<sup>2</sup>). These two transitions are the perfect follow-up for this search, because their excitation

is lower than that of the 220 GHz line and their rest frequencies are well known. In addition, the CH<sub>2</sub>OHCHO (14<sub>0,14</sub>–13<sub>1,13</sub>) is less affected by line blending with respect to the 1.4 mm one, whereas the (10<sub>1,9</sub>–9<sub>2,8</sub>) line is not contaminated by other spectral emissions. As can be seen in Fig. 1, both transitions have been clearly detected at the expected frequencies. The derived FWHMs are 4.6±0.6 km s<sup>-1</sup> and 7.1±0.2 at 103.67 and 143.64 GHz, respectively. Both values are significantly less than the width of the 1.4 mm line (9.2±0.7 km s<sup>-1</sup>). FWHMs spanning of up to a factor of 2 have also been observed by Halfen et al. (2006) towards the Galactic center. In our case the fact that the line width increases with the energy of the transition could be due to an excitation effect, if the higher energy lines arise from a smaller, more turbulent region. We can hence conclude that we have obtained the first detection of glycolaldehyde outside the Galactic center.

The integrated intensity of the 1.4 mm line,  $\int T_B dv = 201.8 \pm 5.9$  K km s<sup>-1</sup>, is definitely higher with respect to those of the 2.1 mm (4.8±0.1 K km s<sup>-1</sup>) and 2.9 mm (1.0±0.1 K km s<sup>-1</sup>) lines. This is the consequence of the beam dilution effect. Figure 2 shows the maps of the three transitions of CH<sub>2</sub>OHCHO integrated emission as well as the velocity gradient detected in CH<sub>3</sub>CN by Beltrán et al. (2004) towards the center of the hot core. As seen in the maps, the emission of glycolaldehyde comes from the central region, where the millimeter continuum peaks. Our angular resolution at 1.4 mm (1".1×0".5) is sufficient to barely resolve the CH<sub>2</sub>OHCHO emission (bottom-left panel of Fig. 2), thus minimising beam dilution effects. On the opposite, the angular resolution of the 2.1 and 2.9 mm maps,  $\simeq 4''$ – $5''$ , causes a significant beam dilution, thus reducing the measured brightness temperature.

Unlike what has been observed towards the Galactic center (Hollis et al. 2001), the CH<sub>2</sub>OHCHO emission does not have a large spatial scale but is rather concentrated towards the center of the core. In fact, the glycolaldehyde emission has a deconvolved size at the 50% of the peak of the emission of  $\sim 1''.3$  ( $\sim 10300$  AU), which is definitely smaller than that derived from standard HMC tracers, such as e.g. methyl cyanide (Beltrán et al. 2005), which is of  $\sim 2''.4$  ( $\sim 19000$  AU). As a consequence, as shown by the rotational temperature and column density maps (see Fig. 7 of Beltrán et al. 2005), CH<sub>2</sub>OHCHO traces the hottest ( $T \geq 300$  K) and densest ( $n_{\text{H}_2} \geq 2 \times 10^8$  cm<sup>-3</sup>) gas in the surroundings of the newly formed star(s), which is located closer to the peak of the continuum emission.

Given the difference of the angular resolution of the three CH<sub>2</sub>OHCHO maps, the comparison of the different lines has been done by convolving the 1.4 mm and 2.1 mm observations to the 2.9 mm HPBW (5".4×4".4). By using the expressions reported by Hollis et al. (2000), we derived the rotational temperature diagram, finding that the diagram is quite flat, which does not allow to derive the column density from the fit. This is probably due to the high opacity of the CH<sub>2</sub>OHCHO lines. In fact, on the one hand, the brightness temperature

of the 1.4 mm line is quite high ( $\sim 30$  K). On the other hand, after smoothing all maps to the resolution of the 2.9 mm line, the brightness temperature of the three transitions turn out to be very similar. This suggests that all three lines are optically thick. Therefore the beam-averaged column densities obtained from the 2.9 and 2.1 mm lines assuming  $T=300$  K ( $N_{\text{CH}_2\text{OHCHO}} \simeq 3 \times 10^{15} \text{ cm}^{-2}$ ), as well as that derived from the better resolved 1.4 mm transition ( $\sim 10^{17} \text{ cm}^{-2}$ ) should be considered as lower limits. A rough estimate of the  $\text{CH}_2\text{OHCHO}$  abundance has been obtained by using the  $\text{H}_2$  column density determined from the continuum dust emission at 1.4 mm (Beltrán et al. 2004). The estimated abundance is of the order of  $10^{-8}$ . Such a high value is consistent with the abundances found by Requena-Torres et al. (2008) towards the Galactic center.

Besides the detection of glycolaldehyde, we wish to demonstrate not only that its column density is consistent with the predictions of theoretical models, but also that other species involved in the same formation route are detected with column densities compatible with those predicted by the models. One of these is  $\text{HCOOCH}_3$ . It appears that the  $\text{HCOOCH}_3$  line at 220445.79 MHz cannot be used to estimate the column density because the value obtained would be implausibly large ( $N_{\text{HCOOCH}_3} \sim 10^{20} \text{ cm}^{-2}$ ). In fact, according to Turner (1991), transitions of complex molecules associated with small ( $\leq 1 \text{ D}^2$ )  $S\mu^2$ , often exhibit intensities in excess by orders of magnitude with respect to the LTE values based on the large  $S\mu^2$  lines. We thus decided to estimate the  $\text{HCOOCH}_3$  column density using data from Cesaroni et al. (1994) for a transition with  $S\mu^2 = 13 \text{ D}^2$ . The result is listed in Table 1, after correcting the  $\text{HCOOCH}_3$  estimates for the different beam with respect to the  $\text{CH}_2\text{OHCHO}$  observations. For this purpose, the expressions of Requena-Torres et al. (2006) have been used. Following the same approach, the column density of methanol ( $\text{CH}_3\text{OH}$ ; Table 1), another molecule involved in the formation process of glycolaldehyde, has also been collected from the literature (Gibb, Wyrowski, & Mundy 2003). Note that if  $\text{HCOOCH}_3$  and  $\text{CH}_3\text{OH}$  were optically thick, the column densities could be much higher. In the following, we compare the column densities thus estimated (see Table 1) with those obtained from theoretical models.

#### 4. The origin of glycolaldehyde in HMCs

In this section we briefly investigate whether the column densities of glycolaldehyde that we derive are indeed chemically feasible. Our purpose is to investigate whether current chemical models of HMCs can account for the observed abundance of glycolaldehyde in massive star forming regions.

To date, several gas-phase and solid-phase routes of formation for glycolaldehyde have

been proposed (e.g. Sorrell 2001; Jalbout 2007). A possible route of formation is via radical reaction of HCO with methanol or with formaldehyde (or, more likely, via intermediate, e.g.  $\text{CH}_2\text{OH} + \text{HCO}$ , where the first species is a direct product of methanol). While such reactions would be too slow in the gas phase to produce detectable abundances of glycolaldehyde in the HMCs lifetime, the high densities ( $10^7 \text{ cm}^{-3}$ ) of such regions may lead to fast surface reactions: it has been proposed for example Charnley & Rodgers (2005) that such reactions may occur in close proximity via the hot secondary electron generated by the passage of a cosmic ray through the ice, or via photoprocessing of grain mantles by UV starlight which create a high concentration of radicals in the bulk interior of mantles. Grain-grain collisions then provide excess heat causing radical-radical reactions to occur and form large organic molecules (Sorrell 2001). In fact, Bennet & Kaiser (2007) have performed an experiment where methanol and CO ices were irradiated with energetic electrons to mimic the presence of cosmic ray ionizations and found that glycolaldehyde was formed provided that methanol and carbon monoxide are in close proximity in the ices.

For the purpose of this investigation, we will adopt as route of formation of glycolaldehyde surface reactions of HCO,  $\text{H}_2\text{CO}$  and  $\text{CH}_3\text{OH}$ , but we note that these somewhat arbitrary choices do not imply that other routes are not important. Also note that in this simple model, the formation of glycolaldehyde on ices via reactions of HCO with methanol implies intermediate passages (just like the formation of methanol from CO in Viti et al. (2004) which we assume to be fast. As far as the destruction of glycolaldehyde is concerned, gas-phase photodissociation would be highly inefficient in such environments due to the high visual extinctions. Destruction by surface reactions will be taken into account by varying the efficiency of formation. Glycolaldehyde formation via neutral-neutral reactions on the grains will affect the abundances of other HMC species such as  $\text{CH}_3\text{OH}$ , and  $\text{HCOOCH}_3$ .

We have used a published HMC model (Viti et al. 2004) modified to include the formation reactions for glycolaldehyde as well as other surface reactions summarized in Bottinelli et al. (2007) to form complex surface molecules (Table 2). The model already included hydrogenation on grains. We have run a small grid of models where we varied the formation rate coefficients of the reactions forming  $\text{CH}_2\text{OHCHO}$  and related species. Our best fit model is one where the efficiencies of the new reactions listed in Table 2 need not be large (e.g. only  $\sim 2\%$  of CO needs to be converted in  $\text{H}_2\text{CO}$ ). The range of ages indicated by the best fit models is consistent with a typical age for a HMC ( $\sim 10^5$ – $5 \times 10^5$  yr). In absence of any experimental measurements, we do not know whether the efficiencies employed for Reactions 2 and 7 (Table 2) are realistic. Nevertheless, we note that the best fitting models imply reasonably small CO conversion efficiencies and probabilities of formation, probably feasible on surfaces where grains act as catalyst. More specifically both reactions occur among products of hydrogenation of CO hence the necessary mobility is low as all the radicals are already in

close vicinity to each other.

## 5. Conclusions

We report the first detection of glycolaldehyde towards a star forming region, the HMC G31.41+0.31 that is hosting massive young stellar object(s). G31.41+0.31, together with G24.78+0.08 A1, is the only massive core where evidence of infall, rotation, and outflow have been simultaneously detected. The maps of CH<sub>2</sub>OHCHO show that the emission, which is smaller than that derived from standard HMC tracers, is clearly associated with the most central part of the core. This emission traces the hottest ( $\geq 300$  K) and densest ( $\geq 2 \times 10^8$  cm<sup>-3</sup>) gas in the surroundings of the embedded high-mass protostar(s). Therefore we propose glycolaldehyde as an excellent tracer of the innermost regions of HMCs. To detect glycolaldehyde towards other HMCs it is crucial to carry out high-angular resolution observations because the interferometer will filter out the extended emission of other lines that might overlap with glycolaldehyde and affect its detectability.

The detection of glycolaldehyde has also profound implications for the chemistry of star forming regions as it can help to constrain the evolutionary stage of the core, and therefore of the embedded O-B (proto)stars. In fact, we show that, for existing HMC gas-grain chemical models, the age of the HCM has to be a few  $10^5$  yr to reproduce the observed column densities of glycolaldehyde (as well as methyl formate and methanol). In addition, only small amounts of CO ( $\sim 10$ – $15\%$ ) need to be processed on grains, making surface reactions the most feasible route to the formation of glycolaldehyde.

We thank Prof D. A. Williams for helpful discussion as well as a thorough reading of the manuscript. SV acknowledges financial support from an individual PPARC Advanced Fellowship.

## REFERENCES

- Araya, E., Hofner, P., Kurtz, S., Olmi, L., & Linz, H. 2008, *ApJ*, 675, 420
- Beltrán, M. T., Cesaroni, R., Codella, C., Testi, L., Furuya, R. S., & Olmi, O. 2006, *Nature*, 443, 427
- Beltrán, M. T., Cesaroni, R., Neri, R., Codella, C., Furuya, R. S., Testi, L., & Olmi, O. 2004, *ApJ*, 601, L190

- Beltrán, M. T., Cesaroni, R., Neri, R., Codella, C., Furuya, R. S., Testi, L., & Olmi, O. 2005, *A&A*, 435, 901
- Bennett, C. J., & Kaiser, R. I. 2007, *ApJ*, 661, 899
- Bottinelli, S., Ceccarelli, C., Williams, J. P., & Lefloch, B. 2007, *A&A*, 463, 601
- Cesaroni, R., Olmi, L., Walmsley, C. M., Churchwell, E., & Hofner, P. 1994, *ApJ*, 435, L137
- Charnley, S. B., & Rodgers, S. D. 2005, in *Astrochemistry: Recent Successes and Current Challenges*, IAU Symposium S231, eds. D. C. Lis, , G. A. Blake, & E. Herbst, (Cambridge University Press, Cambridge), 237
- Churchwell, E., Walmsley, C. M., & Cesaroni, R. 1990, *A&AS*, 83, 119
- Gibb, A. G., Wyrowski, F., & Mundy, L. G. 2003, in *SFChem 2002: Chemistry as a Diagnostic of Star Formation*, eds. C. L. Curry & M. Fich, (NRC Press, Ottawa), 214
- Halfen, D. T., Apponi, A. J., Woolf, N., Polt, R., & Ziurys, L. M. 2006, *ApJ*, 639, 237
- Hollis, J. M., Lovas, F. J., & Jewell, P. R. 2000, *ApJ*, 540, L107
- Hollis, J. M., Vogel, S. N., Snyder, L. E., Jewell, P. R., & Lovas, F. J. 2001, *ApJ*, 554, L81
- Jalbout, A. F. 2007, *Molecular Physics*, 105, 941
- Olmi, L., Cesaroni, R., & Walmsley, C. M. 1996, *A&A*, 307, 599
- Requena-Torres, M. A., Martín-Pintado, J., Martín, S., & Morris, M. R. 2008, *ApJ*, 672, 352
- Requena-Torres, M. A., Martín-Pintado, J., Rodríguez-Franco, A., Martín, S., Rodríguez-Fernández N. J., & de Vicente, P. 2007, *ApJ*, 971, 455
- Snyder, L. E., Lovas, F. J., Hollis, J. M., Friedel, D. N. et al. 2005, *ApJ*, 619, 914
- Sorrell, W. H. 2001, *ApJ*, 555, L129
- Turner, B. E. 1991, *ApJS*, 76, 617
- Viti, S., Collings, M. P., Dever, J. W. McCoustra, M. R. S., & Williams, D. A. 2004, *MNRAS*, 354, 1141



Table 1: Source-averaged column densities towards the G31.41+0.31 HMC.

$\text{CH}_2\text{OHCHO}^{\text{a}}$	$\text{HCOOCH}_3^{\text{a}}$	$\text{CH}_3\text{OH}^{\text{b}}$
( $\text{cm}^{-2}$ )	( $\text{cm}^{-2}$ )	( $\text{cm}^{-2}$ )
$>1 \times 10^{17\text{c}}$	$3.4 \times 10^{18\text{d,e}}$	$7.5 \times 10^{17\text{e}}$

<sup>a</sup>Assuming a kinetic temperature of 300 K, as measured by Beltrán et al. (2005).

<sup>b</sup>From Gibb, Wyrowski, & Mundy (2003).

<sup>c</sup>From the  $\text{CH}_2\text{OHCHO}$  ( $20_{2,18}$ – $19_{3,17}$ ) data.

<sup>d</sup>From the  $\text{HCOOCH}_3$ -E ( $9_{6,3}$ – $8_{6,2}$ ) (110652.89 MHz;  $E_{\text{u}}=51$  K) data of Cesaroni et al. (1994).

<sup>e</sup>In case of optically thick emission, the column densities could be higher.

Table 2: List of reactions added to the Viti et al. (2004) model. “M” denotes species in the solid phase.

$N$	Reaction
1	$\text{CO} + 4(\text{MH}) \Rightarrow \text{MCH}_3\text{OH}$
2	$\text{CO} + \text{MCH}_3\text{OH} \Rightarrow \text{MHCOOCH}_3$
3	$\text{H}_2\text{CO} + \text{MH} \Rightarrow \text{MCH}_3\text{O}$
4	$\text{MCH}_3\text{O} + \text{MHCO} \Rightarrow \text{MHCOOCH}_3$
5	$\text{CO} + 2(\text{MH}) \Rightarrow \text{MH}_2\text{CO}$
6	$\text{CO} + \text{MH} \Rightarrow \text{MHCO}$
7	$\text{MH}_2\text{CO} + \text{MHCO} + \text{MH} \Rightarrow \text{MCH}_2\text{OHCHO}$

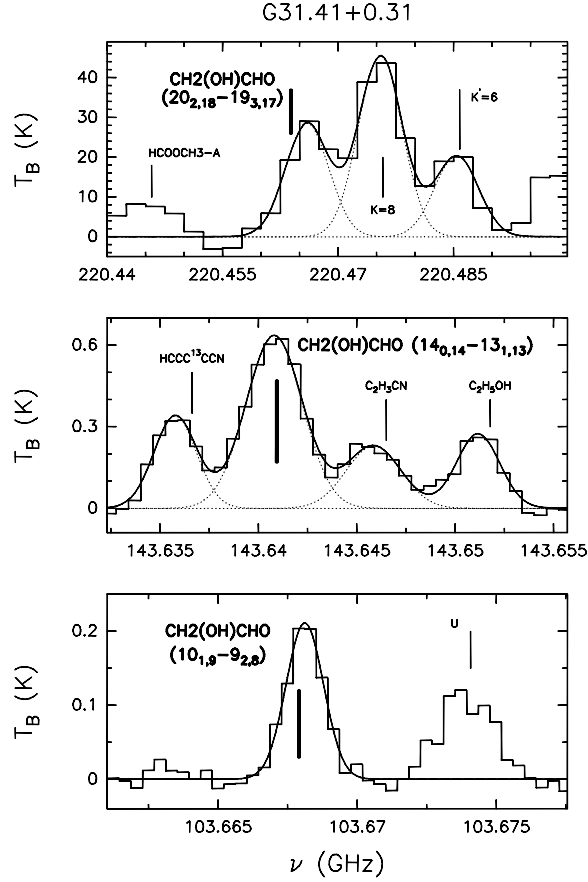


Fig. 1.— Beam-averaged spectra in  $T_B$  scale of the  $\text{CH}_2\text{OHCHO}$  ( $20_{2,18}$ – $19_{3,17}$ ), ( $14_{0,14}$ – $13_{1,13}$ ), and ( $10_{1,9}$ – $9_{2,8}$ ) at 220463.87, 143640.94, and 103667.91 MHz, respectively, as observed towards the central position of the G31.41+0.31 hot core. Rest frequencies are pointed out by vertical bars. *Upper panel* (from Beltrán et al. 2005): The glycolaldehyde line is blended with the  $\text{CH}_3\text{CN}$  ( $12$ – $11$ ;  $K=8$ ) line. Two additional lines are present: (i)  $^{13}\text{CH}_3\text{CN}$  ( $12_6$ – $11_6$ ; labeled by  $K'$ ), and (ii)  $\text{HCOOCH}_3$ –A ( $25_{11,15}$ – $26_{9,18}$ ) (220444.79 MHz;  $E_u=272$  K) which could contain an emission contribution due to the  $\text{CH}_2\text{OHCHO}$  ( $18_{4,14}$ – $17_{4,13}$ ) (220433.51 MHz;  $E_u=108$  K) line. The continuous line shows the fit to the group of three lines formed by the  $\text{CH}_2\text{OHCHO}$  ( $20_{2,18}$ – $19_{3,17}$ ),  $\text{CH}_3\text{CN}$  ( $12$ – $11$ ;  $K=8$ ) and  $^{13}\text{CH}_3\text{CN}$  ( $12$ – $11$ ;  $K'=6$ ); dotted lines draw the three individual Gaussian curves used for the fit. *Middle panel*: The  $\text{CH}_2\text{OHCHO}$  line is part of a spectral pattern containing also the  $\text{HCCC}^{13}\text{CCN}$  ( $54$ – $53$ ) (143636.63 MHz;  $E_u=183$  K),  $\text{C}_2\text{H}_3\text{CN}$  ( $33_{2,31}$ – $32_{4,28}$ ) (143646.50 MHz;  $E_u=620$  K), and  $\text{C}_2\text{H}_5\text{OH}$  ( $29_{2,28}$ – $28_{3,26}$ ) (143651.78 MHz;  $E_u=415$  K) lines. The results of the fit as drawn as in the Upper panel. *Lower panel*: Besides the glycolaldehyde emission, an unidentified spectral pattern is present around 103674 MHz. Solid curve shows the fit of the isolated  $\text{CH}_2\text{OHCHO}$  line.

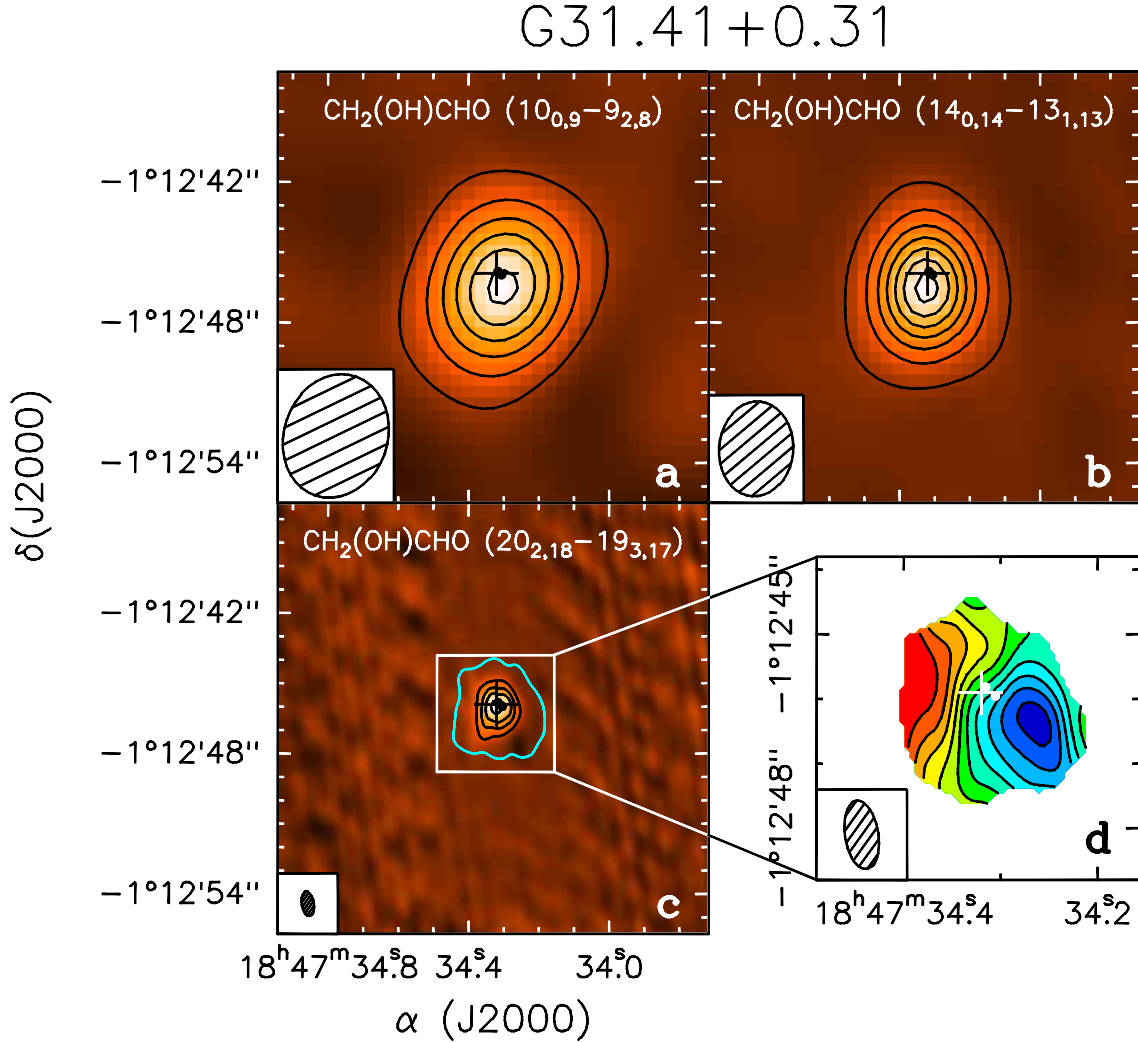


Fig. 2.— Map of the intensity integrated under the  $\text{CH}_2\text{OHCHO}$  ( $10_{0,9}-9_{2,8}$ ) line at 103.67 GHz (a), the  $\text{CH}_2\text{OHCHO}$  ( $14_{0,14}-13_{1,13}$ ) line at 143.64 GHz (b), and the  $\text{CH}_2\text{OHCHO}$  ( $20_{2,18}-19_{3,17}$ ) line at 220.46 GHz (c), towards the hot molecular core G31.41+0.31. The  $3\sigma$  contour of the  $\text{CH}_3\text{CN}$  (12–11) emission averaged under the  $K=0, 1$ , and 2 components is shown in light blue. (d) Close-up of the central region that shows the velocity field of the toroid in G31.41+0.31 mapped by Beltrán et al. (2004). The cross marks the position of the 1.4 mm radio continuum source, and the dots the 7 mm radio continuum sources (Araya et al. 2008). The synthesized beam is shown in the bottom left. The contour levels are: (a) from 0.01 to 0.09 in steps of 0.02  $\text{Jy beam}^{-1}$ ; (b) from 0.04 to 0.52 in steps of 0.08  $\text{Jy beam}^{-1}$ ; and (c) from 0.10 to 0.94 in steps of 0.12  $\text{Jy beam}^{-1}$ .